Journal of Medicinal Chemistry

Article

pubs.acs.org/jmc

Development of Cyclic NGR Peptides with Thioether Linkage: Structure and Dynamics Determining Deamidation and Bioactivity

Kata Nóra Enyedi,[†] András Czajlik,[‡,§] Krisztina Knapp,[∥] András Láng,[⊥,▽] Zsuzsa Majer,[∥] Eszter Lajkó,[▲] László Kőhidai,[▲] András Perczel,[⊥,▽] and Gábor Mező*[,†]

[†]MTA-ELTE Research Group of Peptide Chemistry, Hungarian Academy of Sciences, [▽]MTA-ELTE Protein Modelling Research Group, Hungarian Academy of Sciences, [∥]Laboratory for Chiroptical Structure Analysis, Institute of Chemistry, and [⊥]Laboratory of Structural Chemistry and Biology, Institute of Chemistry, Eötvös Loránd University, Pázmány P. sétány 1/A, 1117 Budapest, Hungary

[‡]Faculty of Information Technology, Pázmány Péter Catholic University, Práter u. 50/A, 1083 Budapest, Hungary

[§]MTA-TTK-NAP B - Drug Discovery Research Group − Neurodegenerative Diseases, Institute of Organic Chemistry, Research Center for Natural Sciences, Hungarian Academy of Sciences, Magyar tudósok körútja 2, 1117 Budapest, Hungary

[▲]Department of Genetics, Cell and Immunobiology, Semmelweis University, Nagyvárad tér 4, 1089 Budapest, Hungary

Supporting Information

ABSTRACT: NGR peptides that recognize CD13 receptors in tumor neovasculature are of high interest, in particular due to their potential applications in drug targeting. Here we report the synthesis and structural analysis of novel thioether bond-linked cyclic NGR peptides. Our results show that their chemostability (resistance against spontaneous decomposition forming *iso*Asp and Asp derivatives) strongly depends on both sample handling conditions and structural properties. A significant correlation was found between chemostability and structural measures, such as $NH^{Gly}-CO^{Asn\text{-}sc}$ distances. The side-chain orientation of Asn is a key determining factor; if it is turned away from HN^{Gly}, the chemostability increases. Structure stabilizing factors (e.g., H-bonds) lower their internal dynamics, and thus biomolecules become even more resistant against spontaneous decomposition. The effect of cyclic NGR peptides on cell adhesion was examined in A2058 melanoma cell lines. It was found that some of the investigated peptides gradually increased cell adhesion with long-term characteristics, indicating time-dependent formation of integrin binding *iso*Asp derivatives that are responsible for the adhesion-inducing effect.

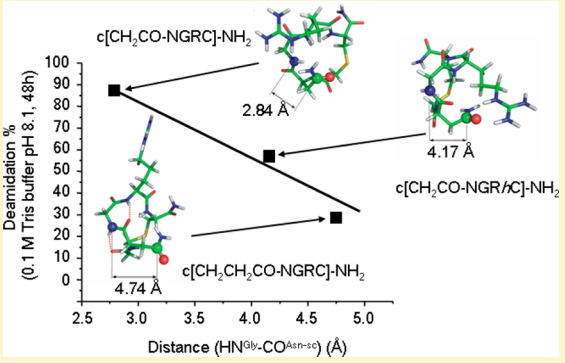

INTRODUCTION

Attention turned to NGR (Asn-Gly-Arg) peptides when non-RGD (Arg-Gly-Asp) integrin-binding motifs were searched via phage-display libraries.[1,2] The NGR motif was the most frequent one among those that showed integrin-binding properties. NGR sequence-containing peptides were also selected as tumor vasculature homing peptides from an in vivo phage-display screening assay on human breast carcinoma xenograft-bearing nude mice.[3] However, this study also indicated that the cyclic ACDC**RGD**CFC peptide (RGD-4C containing 1−4 and 2−3 disulfide bridge isomers) did not compete with the C**NGR**C (NGR-2C) cyclic peptide in tumor-homing properties and vice versa. Later, aminopeptidase N (APN or CD13) was recognized as the receptor that binds NGR peptides.[4] CD13, a membrane-bound metallopeptidase, is not (or is barely) expressed on endothelium of normal blood vessels, but it is upregulated in angiogenic blood vessels and has multiple functions (e.g., protein degradation, cell proliferation, cell migration, angiogenesis).[4−6] Furthermore, CD13 is also expressed by various cell types (e.g., liver, prostate, kidney) in healthy individuals. However, it has been shown by the aid of different anti-CD13 monoclonal antibodies that the immunoreactivities of CD13-containing tumor and normal endothelial cell lines are markedly different.[5,7] This result might originate from different glycosylation patterns and/or receptor isoform conformations. This observation makes CD13 a suitable target for specific targeted delivery of drugs and nanoparticles to tumor neovasculature, by use of NGR peptides as a homing motif.[8,9]

It is well-known that Asn deamidation through succinimide ring formation can easily occur, especially if Asn is followed by Gly on its C-terminus.[10,11] This nonenzymatic intramolecular reaction finally leads to the formation of isoaspartyl (*iso*Asp) and aspartyl (Asp)-containing peptides at about 3:1 ratio and depends on pH, temperature, solvent dielectric constant, amino acid sequence, and secondary structural motifs.[10−19] This modification causes difficulties in the interpretation of in vitro

Received: October 22, 2014
Published: February 3, 2015

DOI: 10.1021/jm501630j
J. Med. Chem. 2015, 58, 1806−1817

and in vivo biological data, as well as in NGR peptide formulation.[20] Furthermore, this nonenzymatic post-translational modification could be responsible for the integrin-binding properties of NGR-containing peptides and proteins. It has been found that cyclic and linear peptides with the *iso*Asp-Gly-Arg sequence can bind to $\alpha_v\beta_3$, $\alpha_v\beta_5$, $\alpha_v\beta_6$, $\alpha_v\beta_8$ and $\alpha_5\beta_1$ integrins, while peptides with the Asp-Gly-Arg sequence do not.[19] Therefore, stability studies of linear and cyclic NGR peptides used as tumor-homing motives are crucial before such drug delivery systems are developed.

At present, a few linear and cyclic NGR peptides have been used for ligand-directed delivery of various drugs and particles to tumor vessels, in an attempt to increase their anti-tumor activity.[7] Cyclic and/or linear peptides containing either c[CNGRC] or GNGRG motif were described as appropriate target ligands in the delivery of tumor necrosis factor α (TNFα),[5,21,22] interferon γ (IFNγ),[23−25] liposomal doxorubicin,[26,27] and Pt complex,[28,29] as well as metal radioisotope-labeled derivatives for positron emission tomography (PET) or single-photon-emission computed tomography (SPECT).[30,31] Upon comparing c[CNGRC] and GNGRG, a cyclic and a linear peptide, not only was higher CD13 binding affinity of the cyclic variant detected but also increased stability in phosphate-buffered saline (PBS; half-lives were 6−8 h and 3−4 h, respectively at pH 7.3 and 37 °C) and in serum (5 and 3 h, respectively).[19] However, efficient formation of disulfide bridges after incorporation of linear NGR peptide onto the surfaces of liposomes or other nanoparticles used for drug targeting is not an easy task. Therefore, to date mainly the less chemostable linear NGR peptides have been used for active targeting of anti-cancer drugs encapsulated by nanoparticles.[32] Negussie et al.[33] successfully developed a head-to-side-chain cyclic NGR peptide. In the c[KNGRE]-NH_2 construct, the amide bond used for cyclization was formed between the N-terminal α-amino group and the side-chain carboxyl group of Glu by on-resin cyclization. The resulted ring size of the 17-atom-containing macrocycle was identical to that of c[CNGRC] with disulfide bond. Their goal was to investigate an NGR homing motif with increased stability for delivery of free or liposome-encapsulated drugs. In this way, the formation of disulfide bonds between adjacent peptides on the liposome surface, which would render the ligand ineffective, could be avoided.[34] The free ϵ-amino group of Lys was used for the attachment of Oregon Green fluorescent label on the liposome, and this did not influence the binding to CD13. The c[KNGRE]-NH_2 ligand displayed 3.6-fold higher affinity for CD13-positive cancer cells than the linear KNGRG. However, the deamidation of these analogues was not investigated in that study.

Since the intact cyclic NGR peptides could bind to CD13, deamidation resulting in aspartyl and isoaspartyl derivatives might restrict the application of cyclic NGR peptides as successful tumor-homing moieties. Nevertheless, the formed *iso*Asp derivatives could be responsible for integrin binding; integrins are also overexpressed in several types of tumors.[35] Therefore, appropriate cyclic NGR peptide conjugates might be dual-acting derivatives through both CD13 and integrin receptors.[36]

In one of our previous studies, it has been shown that the enzymatic and serum stability of a cyclic epitope peptide could be increased when thioether linkage was used instead of amide or disulfide bond.[37] Furthermore, chloroacetylated peptides with orthogonal protecting groups on two cysteines were suitable for cyclization and conjugation to a carrier via thioether bond formation in both cases.[38]

In agreement with the observations described above, in the study reported here we aimed (a) to develop novel thioether bond-linked cyclic NGR peptides of different ring sizes (15−18 atoms in the cycle); (b) to study the structure−stability (rate of deamidation) relationship of these compounds; (c) to evaluate the rearrangement of NGR to *iso*DGR by measuring the time-dependent effect on cell adhesion of A2058 melanoma cell line, as an essential functional index of integrin receptor-mediated tumor targeting; and (d) to compare the data with the results obtained for cyclic Ac-c[CNGRC]-NH_2 and c[KNGRE]-NH_2 derivatives previously reported in the literature.

RESULTS

Synthesis of Cyclic NGR Peptides. In order to synthesize cyclic NGR peptides containing amide, disulfide, and thioether bonds, their linear precursors were first prepared on Rink-Amide MBHA resin via Fmoc/tBu strategy. Cyclization was then carried out in solution.

(1) For preparation of the cyclic peptide containing an amide bond, a Glu derivative was introduced to the C-terminus of the NGR sequence and a Boc-Lys(ClZ)-OH amino acid derivative was attached to its N-terminus. The standard trifluoroacetic acid (TFA) cleavage resulted in semiprotected H-Lys(ClZ)-Asn-Gly-Arg-Glu-NH_2, which was subsequently cyclized: the amide bond was formed between the N-terminus and the side chain of Glu by use of BOP/HOBt coupling reagents. Finally, the ClZ protecting group was removed with liquid HF before HPLC purification of c[KNGRE]-NH_2 (**1**).

(2) The cyclic NGR peptide (Ac-c[CNGRC]-NH_2, **2**) containing a disulfide bond was designed by placing two Cys at both ends of -NGR- and subsequently acetylated at its N-terminus. The disulfide bridge was formed either by use of a trityl SH-protecting group for Cys, with the residue removed by TFA and cyclized under slightly alkaline conditions (0.1 M Tris buffer, pH 8.1, for 24 or 48 h), or by use of Acm SH-protection for cysteines, completed with a cyclization in TFA in the presence of $Tl(tfa)_3$. Deamidation and formation of *iso*Asp-containing peptide were observed under alkaline conditions; the longer reaction time resulted in higher yield of *iso*Asp-containing peptide. On the contrary, under acidic conditions no deamidation of Asn was observed, resulting in the highest yield of **2**.

(3) For preparation of cyclic NGR peptides with thioether linkage, a cysteine was incorporated at the C-terminus of the NGR sequence, while the N-terminus was modified with α- or β-haloacyl group. Chloroacetylated XNGRC peptides (X = Ø, Lys, or Pro) were cyclized in 0.1 M Tris buffer (pH 8.1); the reactions were completed almost quantitatively within 3 h. Only moderate deamidation was detected under these reaction conditions, yielding compounds **3**−**5** {c[CH_2CO-XNGRC]-NH_2: X = Ø (**3**), Lys (**4**), or Pro (**5**)}. Unlike the two cyclic compounds mentioned above (**1** and **2**), both having a total of 17 atoms in the macrocycle, **3** contains 15 atoms while **4** and **5** contain 18 atoms within the macrocycle.

(4) A "methylene elongated" derivative of **3** (c[CH_2CH_2CO-NGRC]-NH_2, **6**) was designed to contain 16 atoms within the macrocycle, closing the NGR subunit within a ring. Reaction of the protected parent NGRC peptide on the solid support with β-halopropionic acid (chloro or bromo) did not result in complete modification of the N-terminal amino group. Since cyclization of the chloroacylated derivative was slow, a

DOI: 10.1021/jm501630j
J. Med. Chem. 2015, 58, 1806−1817

significant amount of the product was converted into *iso*Asp-containing derivative. The latter side reaction was less pronounced for the bromoacylated derivative, as cyclization was completed in less than 3 h and thus the compound was not exposed to alkaline conditions for a long time.

(5) Finally, as the N-terminal chloroacetylation of the parent linear peptide was straightforward, compared to the attachment of *β*-halopropionyl group, the thioether bond formation was achieved as follows. A *homo*Cys was incorporated at the C-terminus of the NGR parent peptide, its N-terminus was chloroacetylated, and the cyclization was completed in 3 h (0.1 M Tris buffer, pH 8.1). c[CH_2CO-NGR*h*C]-NH_2 (**7**) containing 16-atom cycle was synthesized with a much better yield (37.9%) than by the previous strategy via the bromopropionylated precursor, employed for preparation of **6** (17.1%) (note that application of *γ*-bromobutyric acid for formation of the 17-membered ring closed by a thioether bond was unsuccessful). The chemical characteristics of the cyclic peptides are summarized in Table 1, and the HPLC chromatograms and mass spectra of the purified cyclic peptides are presented in Supporting Information (Figure S1). The purity of the cyclic peptides was over 95% in all cases.

Table 1. Analytical Characteristics of Cyclic NGR Peptides[a]

compd	yield (%)	R_t[b] (min)	MW_{calc}[c]	MW_{found}[d]
c[KNGRE]-NH_2, **1**	46.2	12.0	583.3	583.4
Ac-c[CNGRC]-NH_2, **2**	45.3 (36.1, 19.7)[e]	15.8	590.2	590.4
c[CH_2CO-NGRC]-NH_2, **3**	59.1	13.2	487.2	487.4
c[CH_2CO-KNGRC]-NH_2, **4**	62.3	12.7	615.4	615.8
c[CH_2CO-PNGRC]-NH_2, **5**	59.4	15.3	584.2	584.4
c[CH_2CH_2CO-NGRC]-NH_2, **6**	17.1 (7.0)[f]	13.0	501.2	501.3
c[CH_2CO-NGR*h*C]-NH_2, **7**	37.9	13.3	501.2	501.3

[a]Analytical RP-HPLC chromatograms and mass spectra are shown in Supporting Information. [b]HPLC column: Phenomenex Luna (250 mm × 4.6 mm) with 5 μm silica (100 Å pore size); eluents 0.1% TFA/water (A) and 0.1% TFA/CH_3CN−water (80:20 v/v) (B); gradient 0 min 0% B, 5 min 0% B, 50 min 90% B; flow rate 1 mL/min; detection: 214 nm. [c]Monoisotopic molecular weight. [d]ESI-MS: Bruker Daltonics Esquire 3000+ ion trap mass spectrometer. [e]Total yields in case of cyclization with $Tl(tfa)_3$ or by air oxidation for 24 or 48 h (in parentheses). [f]Total yields in case of cyclization from bromo or chloro (in parentheses) derivative of precursor peptide.

Chemostability of Cyclic NGR Peptides. The stability of cyclic NGR peptides was determined under three different experimental conditions: (i) their lyophilized form was stored at 4 °C; (ii) they were dissolved in pure water and in different buffers that are relevant for further synthetic work, such as drug conjugation at 25 °C (room temperature); and (iii) they were incubated in a cell culture medium at 37 °C. The reactions were followed by analytical RP-HPLC and the decomposition was calculated from AUC (area under the curve). The compounds were identified by mass spectrometric analyses and by the aid of reference peptides containing Asp derivative instead of Asn. None of these cyclic NGR peptides, **1**−**7**, decomposed under storage for about 6 months. In addition, they were found to be stable in distilled or slightly acidic water (eluent A used for HPLC) at room temperature for about 48 h. Before summarizing further stability studies, it has to be mentioned that in the case of Pro-containing derivative (**5**), the aspartyl cyclic peptide was the main deamidated product instead of the isoaspartyl one. The exact amount of *iso*Asp derivative formed from **5** could not be exactly determined (in particular, in cell culture medium), because it appeared as a broad shoulder of **5**, which could not be baseline-separated. The stability of the cyclic peptides was also studied in three different buffers (results are summarized in Table 2 and chromatograms are presented in Supporting Information).

(1) In 0.2 M NH_4OAc buffer at pH 5, compounds **1** and **2** did not change at all, while a small amount of decomposed products (1−4%) was observed for compounds **4**−**7** after 48 h. In contrast to the above-mentioned compounds, **3** (the HPLC chromatogram of pure **3** is presented in Figure 1A), the tightest macrocycle containing 15 atoms within the ring, decomposed even under slightly acidic conditions. After 24 h, the Asn/*iso*Asp/Asp ratio was 85/12/3 and the ratio of deamidated compounds increased with time (Table 2, Figure 1B).

(2) In PBS solution at pH 7.4, **1** was completely stable, while **2** and **6** show slightly lower stability. Interestingly, **5**, which contains a Pro, decomposed faster (25% deamidated derivatives of Asn were observed after 48 h), while **4** and **7** deamidated even faster (>50% deamidated compounds after 48 h). Under these conditions, **3** was the most sensitive: after 24 h about 64%, and after 48 h about 85%, of the starting material was modified (Figure 1C).

(3) In 0.1 M Tris buffer, pH 8.1, the decomposition was generally more pronounced. While **1** was still stable, **2** decomposed faster than under neutral conditions (∼85% and ∼71% intact cyclic NGR peptide was observed after 24 and 48 h, respectively). A similar deamidation rate was determined for

Table 2. Chemostability of Cyclic NGR Peptides Determined by HPLC

compd	ratio of Asn-/*iso*Asp-/Asp-containing cyclic peptides[a]			
	0.2 M NH_4OAc, pH 5.0	PBS solution, pH 7.4	0.1 M Tris, pH 8.1	DMEM
c[KNGRE]-NH_2, **1**	100/0/0	100/0/0	100/0/0	54/39/7 (92/7/1)
Ac-c[CNGRC]-NH_2, **2**	100/0/0	93/5/2 (96/3/1)	71/21/8 (85/11/4)	0/72/28 (46/38/16)
c[CH_2CO-NGRC]-NH_2, **3**	67/26/7 (85/12/3)	15/68/17 (36/51/13)	13/69/18 (19/57/24)	(0/68/32)
c[CH_2CO-KNGRC]-NH_2, **4**	90/8/2 (100/0/0)	43/34/23 (58/23/19)	15/52/33 (36/41/23)	(0/64/36)
c[CH_2CO-PNGRC]-NH_2, **5**	98/0/2 (100/0/0)	75/3/22 (86/2/12)	47/5/48 (67/3/30)	*b*
c[CH_2CH_2CO-NGRC]-NH_2, **6**	99/1/0 (100/0/0)	89/8/3 (94/5/1)	73/19/8 (86/10/4)	(0/70/30)
c[CH_2CO-NGR*h*C]-NH_2, **7**	96/3/1 (100/0/0)	44/43/13 (64/28/8)	43/45/12 (66/27/7)	(0/73/27)

[a]The ratio of Asn/*iso*Asp/Asp-containing cyclic peptides was calculated from HPLC chromatograms by use of AUC values. Data correspond to 48 h incubation. Data in parentheses correspond to 24 h incubation. [b]The ratio for **5** cannot be calculated because of the complexity of the HPLC chromatogram (see Supporting Information, Figure S6).

DOI: 10.1021/jm501630j
J. Med. Chem. 2015, 58, 1806−1817

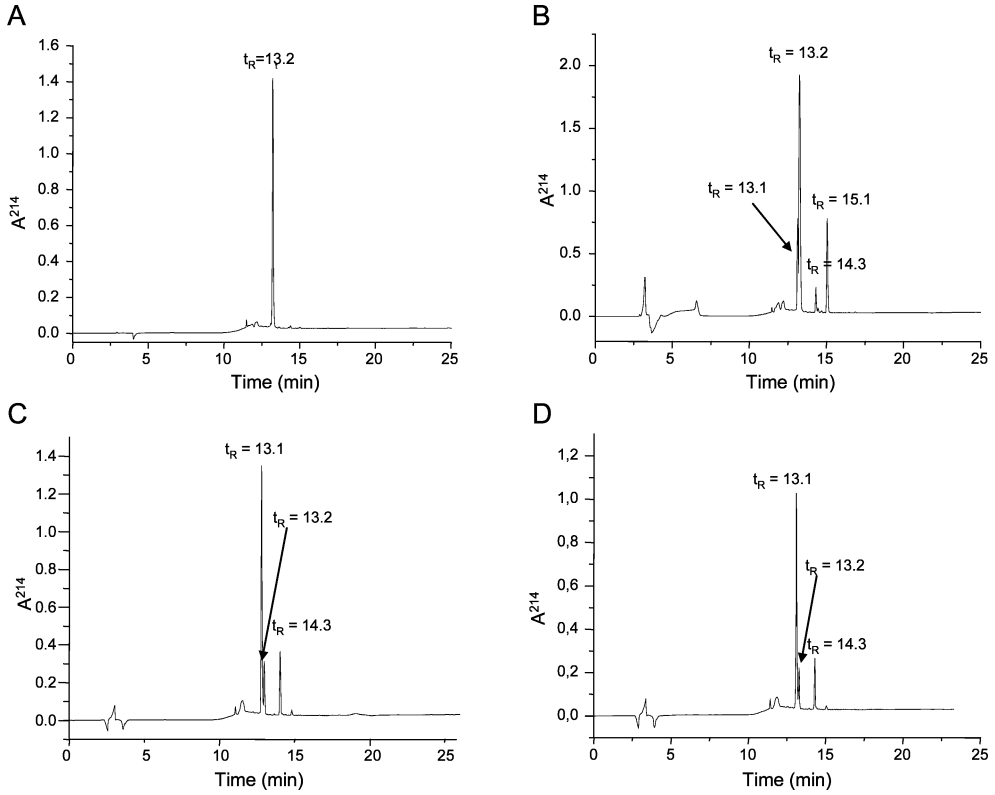

Figure 1. Chemostability determination of c[CH_2CO-NGRC]-NH_2. HPLC chromatograms were recorded after 48 h of incubation at 25 °C in (A) water, (B) 0.2 M NH_4OAc buffer (pH 5.0), (C) PBS solution (pH 7.4), and (D) 0.1 M Tris buffer (pH 8.1). Retention times: 13.2 min corresponds to the intact c[CH_2CO-NGRC]-NH_2, 13.1 min to c[CH_2CO-*iso*DGRC]-NH_2, and 14.3 min to c[CH_2CO-DGRC]-NH_2. Retention time 15.1 min in 0.2 M NH_4OAc buffer corresponds to the Asu derivative.

6 (~73% unmodified **6** after 48 h) and a definitely higher one for **7** (~57% deamidated cyclic peptides after 48 h), only a bit higher than that observed in PBS. Deamidation of **4** in Tris buffer was higher than it was in PBS buffer: ~85% deamidated cyclic peptides after 48 h, which was close to the decomposition of **3** (~87%) under these circumstances (Figure 1D).

(4) In a cell culture medium (pH 7.3 and 37 °C), **1** was fairly stable for shorter time; however, it substantially decomposed afterward (54% of the parent cyclic peptide at 48 h) in a nonlinear manner (Figure 2). More than half of **2** was deamidated after 24 h, and no intact compound was found after 48 h. Cyclic peptides with thioether linkage were also very sensitive in cell culture medium; **3**–**7** decomposed completely during 24 h incubation time.

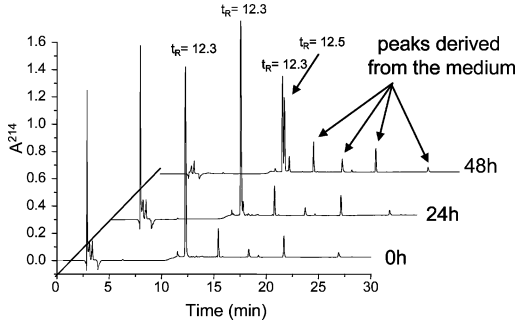

Figure 2. Time-dependent stability of c[KNGRE]-NH_2 in cell culture medium at 37 °C.

Secondary Structure Determination by Electronic Circular Dichroism Spectroscopy. Cyclic pentapeptides often adopt different types of turn conformation (β- and γ-turns). When the amino acid sequence, ring size, and presence of disulfide or thioether linkages is considered, the turn conformation is very probable. The characteristic chiral contributions of different β-turns[39] (C-, C′-, and B-type ECD shape) and γ-turn[40] to the electronic circular dichroism (ECD) spectra has been studied in detail and reviewed and allow their discrimination by ECD spectroscopy. The unstructured conformation (U-type ECD curve) can also be distinguished by ECD.

ECD investigation of the cyclic model peptides in water and TFE (a helix-promoting and membrane-mimicking solvent) can help us understand the conformational stability and solvent sensitivity of peptides; in addition, it can be useful in structure–function investigations.[41] Spectra of **1** were significantly different from all the others (Figure 3). They were characterized by a broad positive band over 200 nm, with maxima at 206 nm (3139.25) and 218 nm (3062.53) in water and at 220 nm (1153.30) in TFE, respectively and a very high intensity negative band below 200 nm [187 nm (−14906.70) in water and 195 nm (−8126.83) in TFE]. The ECD spectra recorded in TFE and water were similar (similar characteristics but higher intensity in water) and indicated a mixture of C′- and B-type pure ECD spectral features.[39]

In TFE, the cyclic compounds **3** and **4** had similar ECD spectra, characterized by a positive band at ~185 nm and a negative band below 200 nm, with a weak negative shoulder at ~225 nm (a mixture of U- and C-type pure ECD curves). In water, the negative bands were more separated, their intensities

DOI: 10.1021/jm501630j
J. Med. Chem. 2015, 58, 1806–1817

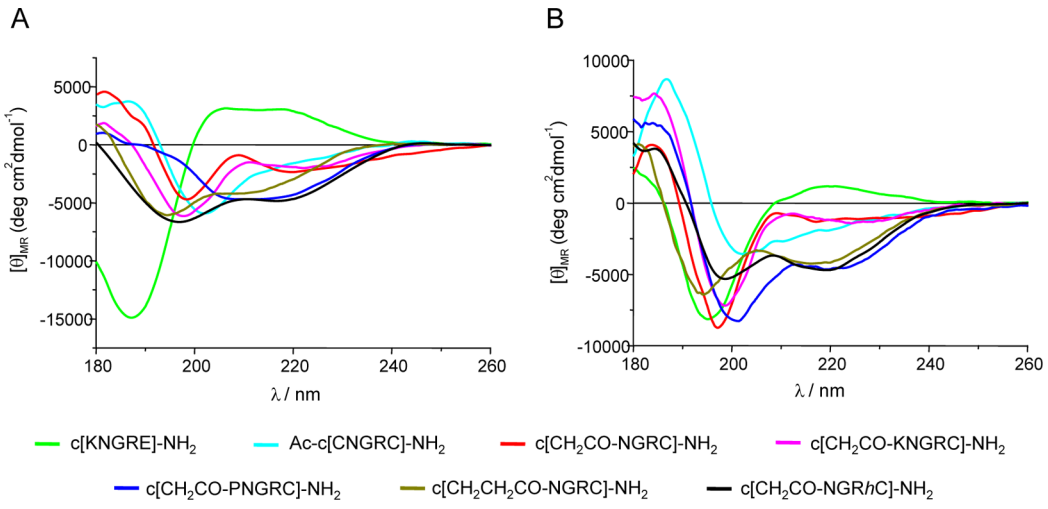

Figure 3. ECD spectra of cyclic NGR peptides **1**−**7** in (A) water and (B) TFE.

were weaker, and the intensity ratio of the longer- and short-wavelength band was changed for both peptides. ECD spectral features of both **3** and **4** indicated elevated backbone flexibility, in agreement with their low chemostability. Compounds **2** and **5** showed typical C-type spectra in TFE. In water, the ECD spectrum of **2** was like the one recorded in TFE, suggesting a higher rigidity, while for **5** the solvent-induced structural changes were a bit more significant: a very broad negative band appeared in the 205−225 nm region.

The ECD spectra of **6** and **7** in the structure-stabilizing solvent TFE showed C-type features, characterized by a positive (∼185 nm) and a negative band (∼200 nm), associated with a negative nπ* shoulder between 220 and 225 nm. In water, the spectrum of both peptides showed two negative broad bands centered at ∼196 and 209 nm (**6**) or 218 nm (**7**). Although ECD spectra cannot reveal high-resolution structural information by using H_2O and TFE solutions, it is obvious that these cyclic NGR peptides have different internal dynamics: some of them have more rigid backbone fold(s) as seen for **1**, **2**, and **5**, while others have probably elevated internal dynamics (e.g., **3** and **4**).

High-Resolution ^{1}H NMR Structures. Distance restraints collected from ^{1}H−^{1}H ROESY spectra (for **1**−**7** in total 106, 97, 87, 122, 107, 79, and 108, respectively) were higher than 20/residue, except for **6**, although most of them were either intraresidual or sequential ones. Medium-range restraints, more indicative of the overall backbone fold(s), were less frequent. This indicated that most of these cyclic peptides had considerable amounts of internal dynamics. In principle, they could adopt several somewhat different backbone conformers in solution at T = 288 K and 3 < pH < 7. No pH-induced structural changes were detected by either ECD or NMR spectroscopy. However, due to the slower exchange rate of the NH resonances, final NMR spectra were recorded at lower pH. In conclusion, we have determined the most prominent and characteristic backbone conformer(s) for each cyclic NGR peptide. Additional minor conformers not resolved at the NMR time scale of motion could, however, be present to some extent, making the conformational ensemble more complex. The side chains, except those of **1**, did not interact with each other or with backbone atoms in a specific manner, and thus they were conformationally diverse.

Structural Coherence of Cyclic Peptides 1−7. Compound **1** has a well-defined backbone structure but not very coherent: backbone and heavy-atom root-mean-square deviation (RMSD) values of $\mathbf{1}^{major}$ are around 0.31 ± 0.23 and 1.13 ± 0.65 Å, respectively (for detailed data for all compounds, see Table S1 in Supporting Information.) The minor conformer of **1**, $\mathbf{1}^{minor}$, distinguished during structure calculations is similar to $\mathbf{1}^{major}$. Unlike for Arg, both φ and ψ torsion angles show larger fluctuation. In spite of its internal dynamics and less coherent structural ensemble, the main conformer, having a γ-turn at Gly, describes well the structural properties of **1** over time. Compound **2** also contains a γ-turn at Gly, with lower RMSDs (0.16 ± 0.20 and 0.75 ± 0.59 Å, respectively).

For **3** an atypical backbone conformer lacking common secondary structural elements was observed, with slightly higher RMSDs (0.36 ± 0.23 and 1.04 ± 0.46 Å, respectively). Nevertheless, the increased internal dynamics (less coherent backbone fold) was in line with the lower chemostability of **3** (it decomposed during NMR measurements 40−50% after a few hours).

The structural properties of **6** and **7** were similar. Although their φ and ψ torsional angles were slightly or, for Asn, even significantly different, their predominant backbone conformers contained γ- and inverse γ-turns (at the -GR- subunits). Although **4** and **5** have a bit larger ring size, closed by a thioether linkage, their RMSDs are also small: 0.09 ± 0.10 and 0.05 ± 0.05 Å, respectively (Table S1, Supporting Information), indicating coherent structural ensembles. However, their 3D structures resemble none of the conformers yet assigned. The latter cyclic NGR peptides tend to form type I β-turns instead of γ- or inverse γ-turns assigned in **1**−**3**, **6**, and **7**. In **5**, two type I β-turns were assigned at the position Pro-Asn as well as Arg-Cys. In contrast, although **4** has almost the same amino acid sequence, it shows an atypical conformer in which only one distorted type I β-turn was found for Lys-Asn. Even though these side chains do not interact in any specific manner, hence keeping their typical flexibility, they are a bit better defined in space: RMSD values ∼0.5 Å.

Critical Distance and Angle Enable Succinimide Ring Formation for the -Asn-Gly- Subunit. For the least chemostable cyclic peptides, prone to form succinimide ring, both a specific Asn side-chain conformation and a sterically preferred NH^{Gly} orientation is needed. The distance between

DOI: 10.1021/jm501630j
J. Med. Chem. 2015, 58, 1806−1817

N^{Gly} and $C(O^{Asn\text{-}sc})$, or d(N−C) for short (Figure 4), could be a characteristic marker of the latter reaction, in line with the most common mechanism described in the literature.[10]

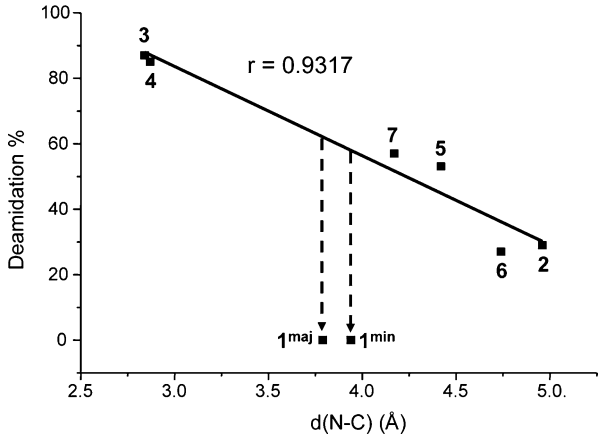

Figure 4. Correlation between distance N^{Gly}−$C(O^{Asn\text{-}sc})$ and deamidation rate 100 × [(*iso*DGR + DGR peptides)/(NGR + *iso*DGR + DGR peptides)] of cyclic NGR peptides **1**−**7** in Tris buffer (pH 8.1) after 48 h.

Macrocycle **3** of the smallest ring size (15 atoms) shows the highest ability to form succinimide ring via spontaneous deamidation. A short d(N−C), ∼2.84 Å, with an N^{Gly}−$C\gamma^{Asn}$−$O\delta^{Asn}$ Bürgi−Dunitz angle[42] ∼ 128°, facilities succinimide ring formation, and thus **3** is the least chemostable cyclic NGR peptide here (Table 3 and Figure 4). The rapid decomposition of **3** is enhanced as its NH^{Gly} is oriented toward the side-chain amide bond of Asn but not H-bonded to the CO of Asn side chain (Figures 5B and 6A). Thus, due to a short d(N−C) (less than the sum of van der Waals radii of the heavy atoms) and the obtuse Bürgi−Dunitz angle, **3** forms isopeptide bond almost quantitatively (∼90%) within 48 h in 0.1 M Tris buffer (note that in **3** no typical NH···CO-type H-bond was assigned).

Compound **4** has similar backbone and side-chain orientations to those found in **3**, especially in its -Asn-Gly-Arg- subunit: -δ_D-δ_L-δ_L- (Table 3).[43] The less optimal Bürgi−Dunitz angle (∼90°) but relatively short d(N−C) (2.87 Å) predicts easy succinimide ring formation for **4**. Once again, no characteristic H-bond stabilizes macrocycle **4**. According to the HPLC analysis (Table 2), **4** decomposes within 48 h in Tris buffer, similarly to **3** (Figure 4). On the contrary, Asn side chain of **2** turns away from the N−H bond of Gly (Figure 6B) and disables N^{Gly} to easily form a succinimide ring: d(N−C) is large (4.96 Å), with a Bürgi−Dunitz angle ∼ 117°. In addition, because of adopting an inverse γ-turn (γ_L, Table 3) of cyclic peptide centered by Asn, a strong backbone H-bond between the NH group of Gly and the carbonyl oxygen of cysteine in position 1 (1.86 Å) could be observed, which reduces the propensity of Asn isomerization. In conclusion, based on its structural properties revealed by ECD and NMR, **2** could be highly resistant against succinimide ring formation and thus against decomposition. Indeed, **2** is a very chemostable peptide (Table 2 and Figure 4); even after 48 h in Tris buffer, the rate of deamidation is lower than 30%. The -Asn-Gly- moiety of **6** forms two γ-turn structures, -γ_L-γ_D- (Table 3), with two robust intramolecular H-bonds, Arg(NH)···Asn(CO) 1.63 Å and Gly(NH)···Prop(CO) 1.82 Å, fixing the backbone of the -NGR- subunit (Figure 5C). The side chain of Asn is turned away, resulting in larger d(N−C) (4.74 Å) and Bürgi−Dunitz angle ∼ 145°, forecasting higher chemical stability. Compound **6** was found by both HPLC and NMR measurements to be reluctant to isomerize: conversion was ∼27% after 48 h in Tris buffer.

Compound **7** has identical ring size as **6** (16 atoms), with -S- at a shifted position. Although the -Gly-Arg- subunit adopts two distorted γ-turns, -γ_D-γ_L- (Table 3), no H-bond stabilizes the backbone of this macrocycle, providing elevated internal dynamics (Figure 5D). The side chain of Asn is still turned away, with d(N−C) = 4.17 Å and Bürgi−Dunitz angle ∼ 106°, but the larger backbone flexibility of **7** makes it more ready for isopeptide formation (conversion close to 60% after 48 h in Tris buffer).

Similarly, in **5** no H-bond(s) stabilizes the backbone structure of the macrocycle, although it encompasses a distorted β-II′-turn structure, -δ_L-α_D- (Table 3). Not only is d(N−C) (4.42 Å) longer and the Bürgi−Dunitz angle ∼ 155° too large but also it contains an H-bond between $NH^{Asn\text{-}sc}$ and $CO^{Asn\text{-}bb}$, d(H···O) ∼1.8 Å. These structural features make **5** a rather stable macromolecule of lower flexibility and thus, it decomposes more slowly than **3**, **4**, and **7** but faster than **2** and **6** (Figure 4).

Compound **1** seems to be the only outlier, as **1** presents two somewhat different conformers, called $\mathbf{1}^{major}$ and $\mathbf{1}^{minor}$, and both forms of **1** (major and minor) have d(N−C) of intermediate length, 3.79 and 3.94 Å, with smaller Bürgi−Dunitz angles ∼ 65° and ∼79°, respectively. Therefore, one would expect **1** to be as chemostable as **7**. By interpolating the recent chemical stability data as a function of d(N−C) (Figure 4), the isopeptide bond formation of **1** is forecasted to be ∼65% (in Tris buffer after 48 h). However, **1** was found to be by far the most chemostable macrocycle: no decomposition was

Table 3. Backbone Conformers of X-NGR-Y Peptides[a]

compd	X	N	G	R	Y	d(N−C), Å	BD angle,[b] deg
c[KNGRE]-NH_2, $\mathbf{1}^{major}$	β_L	α_D	γ_D	γ_L	δ_D	3.79	65.02
c[KNGRE]-NH_2, $\mathbf{1}^{minor}$	ε_L	α_D	γ_D	α_L	α_L	3.94	78.65
Ac-c[CNGRC]-NH_2, **2**	ε_L	γ_L	γ_D	δ_L	γ_L	4.96	117.21
c[CH_2CO-NGRC]-NH_2, **3**		δ_D	δ_L	δ_L	α_L	2.84	127.91
c[CH_2CO-KNGRC]-NH_2, **4**	α_L	δ_D	δ_L	δ_L	δ_L	2.87	89.31
c[CH_2CO-PNGRC]-NH_2, **5**	α_L	δ_L	α_D	α_L	α_L	4.42	155.22
c[CH_2CH_2CO-NGRC]-NH_2, **6**		γ_L	γ_D	α_L	α_D	4.74	145.09
c[CH_2CO-NGR*h*C]-NH_2, **7**		δ_L	γ_D	γ_L	δ_D	4.17	106.33

[a]Representative 3D local folds of the cyclic NGR peptides, depicted by one of the nine typical backbone conformers/amino acid residues α_L, β_L, γ_L, δ_L, ε_L, α_D, γ_D, δ_D, and ε_D as introduced earlier.[43] [b]Bürgi−Dunitz angle = N^{Gly}−$C\gamma^{Asn}$−$O\gamma^{Asn}$.

DOI: 10.1021/jm501630j
J. Med. Chem. 2015, 58, 1806−1817

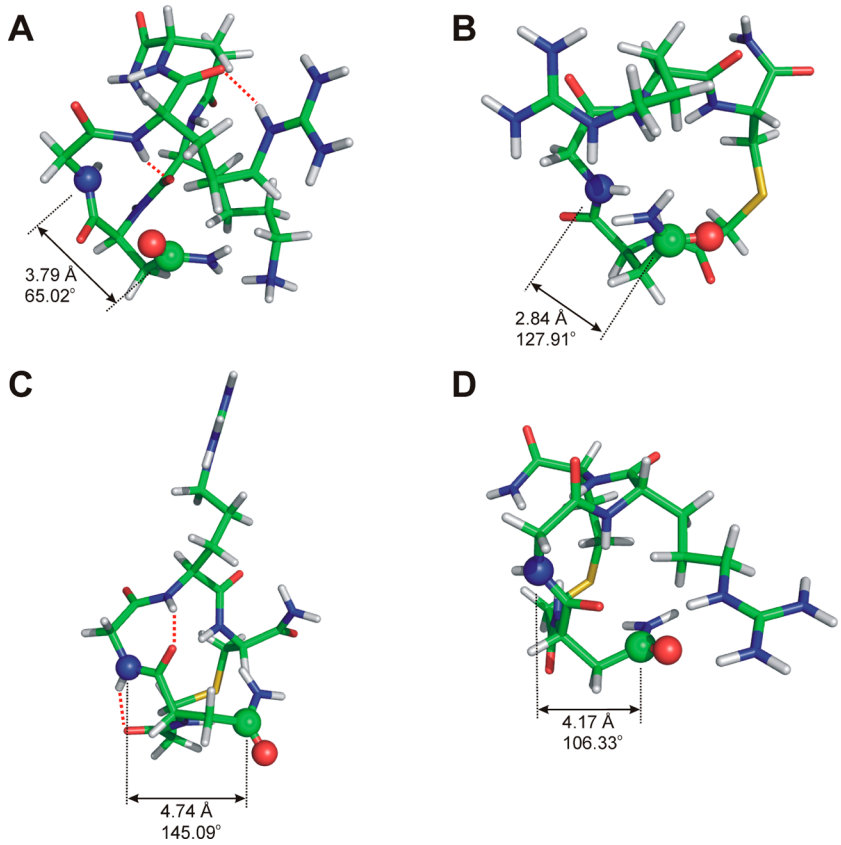

Figure 5. Structures of cyclic NGR peptides (A) $\mathbf{1}^{major}$, (B) **3**, (C) **6**, and (D) **7**, presenting d(N−C) in angstroms and Bürgi−Dunitz angle between N^{Gly} (blue sphere) and $CO^{Asn\text{-}sc}$ in degrees. C is shown as a green sphere and O as a red sphere; H-bonds are shown as dashed red lines.

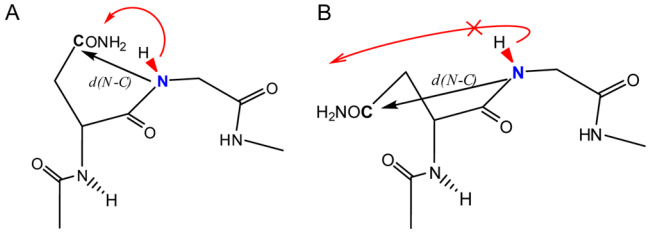

Figure 6. (A) Rapidly decomposing molecules (**3** and **4**), both of low chemostability, have Asn side chain oriented toward NH^{Gly}, faciliting succinimide ring formation. (B) Chemostable compounds (e.g., **2**, **6**) have Asn side chains oppositely oriented, away from NH^{Gly}, making succinimide ring formation difficult. If B-type structures are further stabilized by H-bonds, cyclopeptides are more rigid and succinimide ring formation becomes impossible, as seen for $\mathbf{1}^{major}$ and $\mathbf{1}^{minor}$.

observed (conversion <1% after 48 h in Tris buffer). The question is what structural feature stabilizes **1** and prevent its decomposition. A thorough structural analysis reveals and explains the extreme chemostability of **1** as follows: (1) Both forms of **1** (minor and major) incorporate a type-I′ β-turn (-α_D-γ_D-) at its -Asn-Gly- subunit (Table 3), having Gly in it as a γ-turn. (2) In $\mathbf{1}^{major}$, a strong backbone interaction, $d(NH^{Arg}\cdots CO^{Lys})$ ∼1.6 Å, and a robust backbone−side-chain H-bond, $d(NH^{Arg\text{-}sc}\cdots CO^{Arg})$ ∼1.9 Å, lock the fold in such a way that N^{Gly} cannot attack as a nucleophile from the backside of the molecule (Figure 5A). (3) In $\mathbf{1}^{minor}$, three backbone−side-chain H-bonds [$d(NH^{Glu}\cdots CO^{Glu\text{-}sc})$ ∼1.9 Å, $d(NH^{Arg}\cdots CO^{Asn\text{-}sc})$ ∼2.5 Å, and $d(NH^{Gly}\cdots CO^{Glu\text{-}sc})$ ∼2.4 Å] as well as a robust backbone−backbone H-bond [$d(NH^{Glu\text{-}sc}\cdots CO^{Lys})$ ∼2.6 Å] lock the fold and disable N^{Gly} to attack as a nucleophile.

Thus, in both forms of **1**, complex H-bond networks stabilize the 3D-fold in which Asn is turned away from N^{Gly} and thus disfavors succinimide ring formation. In conclusion, in a flexible backbone fold, if d(N−C) is short and the Bürgi−Dunitz angle is slightly obtuse (∼107°), then isomerization will easily take place. However, the latter rule of thumb holds only if an H-bond(s) does not lock the macrocycle in such a fold where either N^{Gly} cannot be a nucleophile and/or in the vicinity of $CO^{Asn\text{-}sc}$.

Effect of Cyclic NGR Peptides on Cell Adhesion. Formation of *iso*Asp derivatives from -Asn-Gly-containing fragments is expected to be frequent in both in vitro and in vivo systems. According to the literature data, many of the studied cyclic *iso*DGR peptides {e.g., c[C*iso*DGRC]GVRY (*iso*DGR-2C)} show high affinity to $\alpha_v\beta_3$ RGD-binding integrin receptor, in the nanomolar concentration range.[44] However, receptor recognition of *iso*DGR peptides highly depends on their structure.[19,45] Therefore, our objectives were not only to evaluate the 3D structure and chemostability of the cyclic NGR peptides but also to investigate their time-dependent influence on cell adhesion, which might correlate with the amount of formed isoaspartyl derivative. For such a study, cell adhesion was monitored as one of the most significant integrin-dependent properties of metastatic tumorigenesis. The potential effect on cell adhesion was evaluated in A2058 melanoma cell line, by an impedance-based functional assay, for the cyclic NGR peptide-coated surfaces. A2058 cells were selected for this study because it has previously been shown that the chemotaxis, haptotaxis, motility, and migration of A2058 cells are mainly mediated by the $\alpha_v\beta_3$ receptor, highly expressed on their surface.[46]

DOI: 10.1021/jm501630j
J. Med. Chem. 2015, 58, 1806−1817

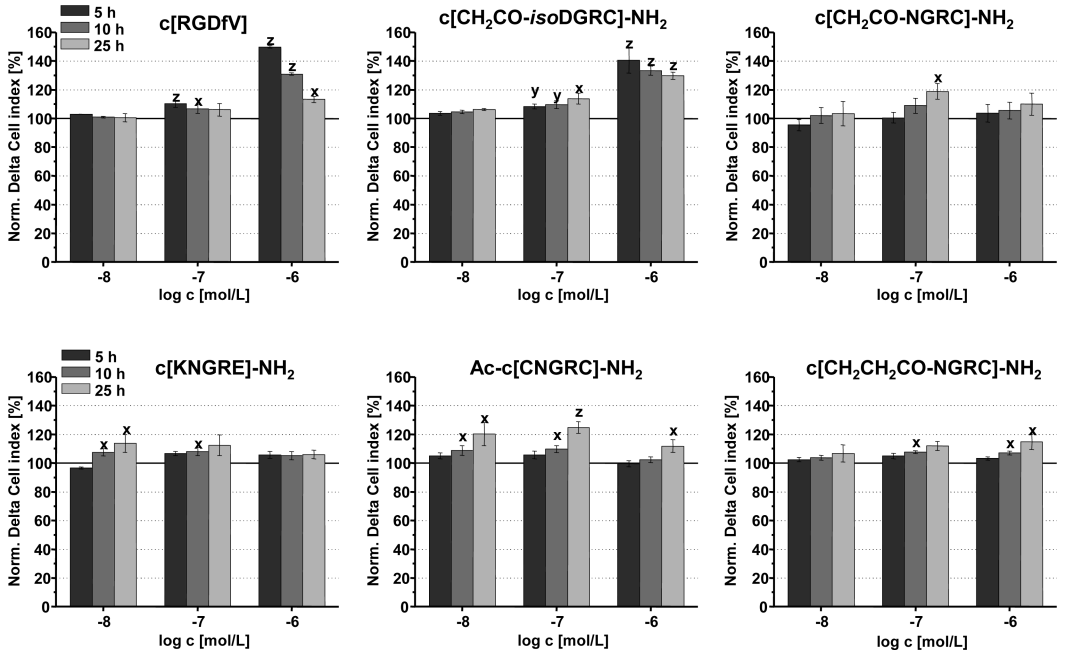

Figure 7. Time-dependent cell adhesion of A2058 melanoma cell line induced by c[RGDfV], c[CH_2CO-*iso*DGRC]-NH_2, and cyclic NGR peptides (**3**, **1**, **2**, and **6**). Normalized change in cell index values (Norm. Delta Cell Index, %) were calculated at individual time points (5, 10, and 25 h) and were normalized to the control (control = 100%). The level of significance is shown as follows: *x*, $p < 0.05$; *y*, $p < 0.01$; *z*, $p < 0.001$.

As described above, rearrangement of the studied cyclic NGR peptides to *iso*Asp is a time-dependent process. Thus, formation of *iso*Asp derivatives having integrin receptor-binding propensities may result in the development of an effect on cell adhesion in time. In contrast to NGR peptides, RGD and *iso*DGR peptides that recognize RGD-binding integrin receptors can influence the cell adhesion in a short period of time. Therefore, c[Arg-Gly-Asp-DPhe-Val] (c[RGDfV]) peptide, which has efficient $\alpha_v\beta_3$ integrin-binding properties, was used as a positive control. To test our hypothesis that the *iso*Asp derivatives have integrin binding activity and therefore can lead to an increased adhesion effect, the most rapidly forming *iso*Asp derivative (c[CH_2CO-*iso*DGRC]-NH_2, derived from **3**) was also screened. The xCELLigence SP system (Roche Applied Science, Indianapolis, IN) used for cell adhesion measurements allowed us to monitor A2058 cell line in a real-time manner (sampling of data in every 20 s) for 25 h.

The c[RGDfV] peptide developed a rapid (in less than 5 h) concentration-dependent adhesion-inducing effect at 10^{-7}–10^{-6} M concentrations, while its effect decreased in the long term (after 10 h). In the case of c[CH_2CO-*iso*DGRC]-NH_2, a concentration and time-dependent adhesion inducer effect was shown, similar to that of c[RGDfV], in the 10^{-7}–10^{-6} M range (Figure 7). Adhesion of A2058 cells incubated with 10^{-6} M c[CH_2CO-*iso*DGRC]-NH_2 reached the maximum level within 5 h and a slight, gradual decline could be detected after 10 h (Figure 7). In contrast, **3** continuously enhanced cell adhesion after 5 h incubation time. At a concentration of 10^{-7} M, **3** led to a significant gradual increase in cell adhesion, with long-term characteristics (Figure 7). A correlation between chemical stability and the effect on cell adhesion was observed in the case of cyclic peptides **1** and **2** containing 17-membered cycle (Figure 7).

Compound **2**, characterized by lower chemostability, continuously enhanced cell adhesion during the incubation time (5–25 h), especially in the 10^{-8}–10^{-7} M concentration range. In the case of **1**, which was fairly stable even in cell culture medium at 37 °C, this effect was moderate (at 10^{-8}–10^{-7} M) or insignificant (at 10^{-6} M). An adhesion inducer effect could also be detected for **6** at 10^{-7}–10^{-6} M and this characteristic became more pronounced at later time points (Figure 7). However, the significance of this effect was less than that of **3**. The other cyclic NGR peptides (**4**, **5**, and **7**) containing a thioether linkage proved to be neutral during the whole period of measurement, in the entire concentration range (data not shown).

DISCUSSION

NGR peptides or their drug conjugates might find important applications in tumor therapy. However, the easy deamidation of NGR peptides, resulting in both *iso*Asp and Asp derivatives, indicates the difficulties in their synthesis and biological experiments. Therefore, stability studies under appropriate circumstances are necessary. We have previously demonstrated that cyclic peptides containing a thioether linkage in the ring are more stable under both chemical and biological conditions than those containing either amide or disulfide bonds.[37] Thus, five new cyclic NGR peptides, all with thioether bonds, were prepared in order to select appropriate constructs for tumor drug-targeting studies. Cyclic peptides of different ring sizes ($15 \leq n \leq 18$ atoms) were designed on the basis of previous studies.[17−19] The smallest ring size ($n = 15$) is **3**, while its elongated derivatives **4** and **5** have the largest ring size ($n = 18$). The later ones were developed on the basis of literature data that suggested them as potential CD13 receptor-binding NGR sequences.[18,33] Furthermore, **4** has a direct conjugation site on the side chain of Lys residue. Preparation of cyclic NGR peptides with 16-atom ring size ($n = 16$) was carried out by methylene elongation within the cycle, using either halopropionic acid instead of acetic acid derivative, in the case of **6**, or incorporation of homocysteine instead of Cys for **7**. They differ

DOI: 10.1021/jm501630j
J. Med. Chem. 2015, 58, 1806−1817

in the position of sulfur atom in the cycle (up to now, no cyclic NGR peptides of 17-membered ring size with thioether linkage have been prepared). In addition, two reference cyclic NGR peptides with amide or disulfide bonds and 17 atoms in the ring (**1** and **2**) that have already been applied for drug targeting were prepared.[33,34] An alternative synthetic route for **1** is proposed here.[33] Synthetic conditions used for disulfide bond formation, as well as their yield, were studied for **2**, and it was found that alkaline conditions for disulfide bond formation should be avoided. In addition, it was found that the chemoselective ligation between the chloroacetyl group and homocysteine (**7**) resulted in significantly higher yield than in the case of halopropionyl group and cysteine (**6**) for synthesis of the same ring size.

Deamidation of NGR peptides via succinimide ring formation, followed by hydrolysis that leads to the formation of both Asp and *iso*Asp derivatives, is well-known. The chemostability of selected cyclic NGR peptides was studied here. Conditions were selected on the basis of applied synthetic routes for cyclization, drug conjugation, or in vitro biological experiments. Because the prepared cyclic NGR peptides without drug molecules will not be tested in further in vivo experiments, their stability in plasma/serum was not investigated within the study reported here. The chemostability of these cyclic peptides with thioether linkage was compared to that of the two reference compounds. As reported in the literature, elevation of pH and/or temperature, as well as use of buffers, increased the decomposition of any cyclic NGR peptide. However, significant differences were found in the rate of succinimide ring formation of the present compounds; namely, the order **1** ≫ **6** ∼ **2** > **5** > **7** > **4** > **3** was established. It is worth mentioning that, after isomerization, the ratio of Asp/*iso*Asp depended on the structure of the compounds. In all cases, the *iso*Asp derivatives were formed in 2−4 times higher amount than the Asp derivatives, except for c[CH_2CO-PNGRC]-NH_2, where the Asp derivative was the main decomposed product.

We have hypothesized that the differences in chemostability have a structural and internal mobility "background". The latter concept was verified by both ECD and NMR spectroscopic analyses. While ECD gives information on the overall folds of these NGR peptides, NMR provides similar information but at the atomic level. On the basis of our results, the following can be concluded: (1) Spatial proximity of Asn side chain to N^{Gly} facilitates succinimide ring formation. (2) In contrast, if N^{Gly} takes part in an H-bond, then decomposition via succinimide ring formation is difficult or impossible. According to NMR data analysis, we conclude that d(N−C), the distance between N^{Gly} and $C\gamma^{Asn\text{-}sc}$ atoms, is a relevant measure of stability rate, and significant correlation was observed between them (Figure 4). (3) However, if Asn side chain is pointing away from N^{Gly} and the molecular fold is locked by H-bonds in the latter conformation, chemostability will be high and the decomposition of NGR will be difficult, as seen for **1**. In PBS, the latter correlation is less pronounced but still significant.

Tumor selectivity, and consequently the drug delivery ability of cyclic NGR peptides, arises from two factors as reported in the literature: (i) NGR peptides bind to CD13 receptor overexpressed on angiogenic endothelium, while (ii) deamidated *iso*DGR derivatives, similarly to RGD peptides, bind to RGD-specific integrin receptors (Figure 8). The in vitro binding efficacy to CD13 receptor cannot be properly characterized in the absence of radiolabeled or fluorescently

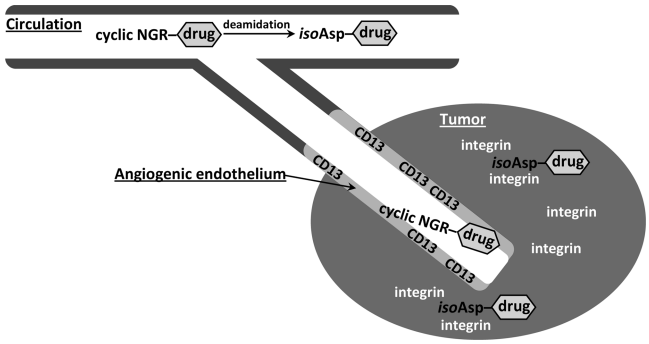

Figure 8. Schematic mode of action of cyclic NGR peptide in targeted drug delivery of tumors.

labeled derivatives. Furthermore, there are only a few cell types (HUVEC and HT-1080 fibrosarcoma) that are available for determining CD13 binding of peptides.[47] Therefore, in a preliminary study, the possible binding of deamidated compounds to integrin receptors was performed by an indirect method. As integrin receptors influence cell adhesion, the binding of *iso*DGR peptides to these receptors might change their adhesive propensity. The results showed that control cyclic peptides such as (c[RGDfV] and the integrin-binding **3**-derived c[CH_2CO-*iso*DGRC]-NH_2 reached the maximum effect on cell adhesion in a short time, while some of the cyclic NGR peptides (**1**−**3** and **6**) increased cell adhesion during the period of experiments (up to 25 h). The increase in time-dependent cell adhesion can be explained by the deamidation process of cyclic NGR peptides, resulting in *iso*Asp derivatives. In the case of **4** and **7**, the absence of an effect on cell adhesion might arise from the lack of binding to integrin receptors. Deamidation of Pro-containing **5** results in Asp and not *iso*Asp derivative, which does not bind to integrin receptors according to literature data.

In conclusion, while chemostable cyclic NGR peptides could be used for drug targeting via CD13 receptors, compounds easily decomposing to form *iso*Asp derivatives might be applied for a dual targeting strategy. Both CD13 and RGD-type integrin receptors could be reached by these molecules during targeted tumor therapy (Figure 8). To elucidate whether this dual targeting approach has any advantage over the application of NGR or RGD peptides alone or in a mixture requires further studies. For this purpose, the present cyclic NGR peptides with thioether linkage are promising candidates to develop drug conjugates for targeted tumor therapy.

■ EXPERIMENTAL SECTION

General Procedures. All solvents and chemicals (Supporting Information) were used as purchased, without further purification. Linear precursor peptides were prepared by Fmoc/^{t}Bu strategy on Rink-Amide MBHA resin (0.5 g, 0.64 mmol/g capacity) according to the protocol described in Supporting Information. Standard Fmoc-amino acid derivatives were used for the syntheses, except for BOC-Lys(ClZ)-OH, which was attached to the N-terminus of linear peptide used for the amide bond containing cyclic peptide **1**. The peptides were cleaved from the resin with a mixture of 95% TFA/2.5% TIS/2.5% water (v/v/v) for 2.5 h at room temperature. The crude products were purified by semipreparative RP-HPLC (experimental conditions are presented in Supporting Information). Purified linear peptides were cyclized as described below, followed by HPLC purification. The cyclic products were analyzed by analytical HPLC and mass spectrometry (Table 1 and Supporting Information). The purity of all compounds was over 95%.

DOI: 10.1021/jm501630j
J. Med. Chem. 2015, 58, 1806−1817

Synthesis of Cyclic Peptide 1 with Amide Bond. Prior to cyclization of linear semiprotected H-Lys(ClZ)-Asn-Gly-Arg-Glu-NH_2, the TFA counterion was exchanged to chloride by use of pyridinium hydrochloride. The cyclization was carried out in *N*,*N*-dimethylformamide (DMF) at a peptide concentration of 0.2 mg/mL, in the presence of BOP/HOBt/DIEA reagents (6:6:12 equiv to peptide) for 24 h. The solvent was evaporated and the remaining oily product was dissolved in eluent A and purified by RP-HPLC. After lyophilization, the purified product was dried further in a desiccator over P_2O_5, and then the ClZ group from the side chain of Lys residue was removed by liquid HF (HF/*p*-cresol =10 mL/1 g).

Synthesis of Cyclic Peptide 2 with Disulfide Bridge. Two methods were applied for disulfide bridge formation. Trityl group was used for side-chain protection of Fmoc-cysteine derivative in the first case. At the end of the synthesis, the N-terminus was acetylated with Ac_2O/DIEA/DMF mixture (1:1:3 v/v/v). The peptide was cleaved from the resin as described above. The cyclization of purified linear peptide was carried out by air oxidation in 0.1 M Tris buffer (pH 8.1) at 0.2 mg/mL peptide concentration for 24 or 48 h. In the second case, Fmoc-Cys(Acm)-OH was applied for the synthesis of linear precursor peptide. For disulfide bridge formation, Ac-Cys(Acm)-Asn-Gly-Arg-Cys(Acm)-NH_2 was dissolved in TFA containing 2% anisole at 0.2 mg/mL peptide concentration, and then 1.2 equiv $Tl(tfa)_3$ was added to the solution. The oxidation reaction was continued for 1 h.

Synthesis of Cyclic Peptides 3−7 with Thioether Linkage. The N-terminus of the peptides was chloroacetylated on resin by use of 5 equiv of chloroacetic acid pentachlorophenyl ester (ClAc-OPcp)[38] or halopropionated with the appropriate halopropionic acid in the presence of equivalent DIC and HOBt coupling agents. The thioether bond was formed in 0.1 M Tris buffer (pH 8.1) as follows: lyophilized pure linear peptides were added to the buffer in portions over 2 h. The final peptide concentration was 10 mg/mL in all cases. The reaction mixtures were stirred for another 1 h.

Stability Studies of Cyclic NGR Peptides. The lyophilized compounds were stable under storage at 4 °C for 6 months. The solution stability of the compounds was evaluated in deiionized (DI) water, in 0.2 M NH_4OAc buffer (pH 5.0), PBS solution (pH 7.4), and 0.1 M Tris buffer (pH 8.1) at a peptide concentration of 1.0 mg/mL (∼2 mM) and room temperature for 48 h. The stability of the compounds was also investigated in DMEM GlutaMAX-I (Sigma, St. Louis, MO) cell culture medium containing 10% FCS (fetal calf serum, Sigma) and gentamicin (160 μg/mL), at the same peptide concentration and 37 °C for 48 h. Decomposition of cyclic NGR peptide derivatives was followed by analytical HPLC.

Structural Studies by Electronic Circular Dichroism Spectroscopy. ECD spectra ($185 < \lambda < 300$ nm) in water and TFE were recorded on a Jasco J-810 spectropolarimeter at T= 298 K in a 0.02 cm quartz cell. Peptide concentration was set to 0.5−1 mg/mL (∼1−2 mM), and each spectrum was the average of five subsequent scans. The recorded spectra were subsequently smoothed by the Means Movement algorithm, and the final ECD band intensities were expressed in mean residue ellipticity ($[\Theta]_{MR}$, deg·cm^2/dmol).

Structural Studies by NMR Spectroscopy. For NMR analysis, samples of all cyclic peptides (∼1 mM) were prepared in H_2O/D_2O mixture (9:1) at pH ∼ 3 and pH ∼ 5. NMR experiments were carried out at 288 K on a Bruker Avance III 700 MHz spectrometer, equipped with 5 mm triple-resonance probe head with *z*-axis pulsed field gradient. Identification of spin systems and sequence-specific assignments were obtained from 2D ^{1}H−^{1}H ROESY (250 and 350 ms), ^{1}H−^{1}H TOCSY (80 ms), and ^{1}H−^{1}H DQF-COSY spectra at 288 K. NMR data processing was performed with the help of TopSpin 3.1 and the spectra were analyzed by use of CCPNMR analysis 2.1 software packages.[48] From the appropriate ROESY spectra, a total of 106, 97, 87, 122, 107, 79, and 108 distance restraints were obtained for cyclic peptides containing NGR motif (**1**−**7**, respectively). For the restraints, three distance ranges (0.18−0.25, 0.25−0.35, and 0.35−0.50 nm) were used, based on the intensity of corresponding ROESY peaks. Structure calculations were performed with the standard simulated annealing protocols by the CNS software package.[49,50] For each compound, an ensemble of 100 structures was calculated and examined. For chemical shift referencing, DSS (2,2-dimethyl-2-silapentane-5-sulfonic acid) was used.

Cells and Culturing. Effects of cyclic NGR peptides on cell adhesion were evaluated on A2058 human melanoma cell line derived from a brain metastasis.[51] This cell line shows high metastatic potency and different substrate-bound, RGD sequence-containing extracellular matrix proteins (e.g., laminin, fibronectin) acting along gradient-induced directional migration (haptotaxis).[46]

Cultures of A2058 were maintained in RPMI 1640 (Sigma, St. Louis, MO) containing 10% FCS (Lonza Group Ltd., Switzerland), L-glutamine (2 mM) (Gibco/Invitrogen Corp., New York), and 100 μg/mL penicillin/streptomycin (Gibco/Invitrogen Corp.) at 37 °C in a humidified 5% CO_2 atmosphere.

Cell Adhesion Assay. The adhesion modulator effect of cyclic NGR peptides on A2058 melanoma cell line was determined on an xCELLigence SP System (Roche Applied Science, Indianapolis, IN). Impedimetric evaluation of cell adhesion was previously described in detail.[52] In brief, the system is a dedicated one to detect the kinetics and strength of cell attachment by monitoring electrical impedance across gold microelectrodes (E-plate) in real time. The measured values (cell index = CI) represent the number and spreading of cells.

Cyclic NGR peptides were tested in 10^{-8}−10^{-6} M concentration range. Consecutive 10-fold dilutions of the peptides were made in 0.1% gelatin (Sigma, St. Louis, MO) dissolved in PBS (phosphate-buffered saline, pH = 7.4). The surface of the electrode in each well of the E-plate was coated by 25 μL of different concentrations of NGR peptides for 20 min at 4 °C. After incubation, the solutions of NGR peptides were removed, and the wells were desiccated for 5 min at room temperature under sterile conditions. To gain a background curve of constant CI value, 100 μL of pure cell culture medium was added to each well and the CI was recorded for 30 min. In the following step, 10^4 cells/well were loaded on the E-plate. The wells coated with 0.1% gelatin solution without test compound served as a control. Cell adhesion of A2058 cells on NGR peptide-coated surface was monitored every 20 s for 25 h at 10 kHz. Each measurement was carried out in triplicate.

The Delta CI (ΔCI) values gained at individual time points (5, 10, and 25 h) were used for data analysis; the integrated software (RTCA 1.2) was applied in calculations. ΔCI refers to the difference in CI value at the time point of cell inoculation and at a given time point. ΔCI values of each concentration of cyclic NGR peptides were normalized to the control and are given as normΔCI in percent.

Statistical Evaluation of Data. Data shown in Figure 7 represent averages expressed as percentage of untreated control ± standard deviation (SD) values. Statistical analysis of data was performed by analysis of variance (ANOVA) with Origin Pro8.0 (OriginLab Corp., Northampton, MA). The level of significance is shown as follows: *x*, $p < 0.05$; *y*, $p < 0.01$; *z*, $p < 0.001$.

■ ASSOCIATED CONTENT

Ⓢ Supporting Information

Additional text describing solid-phase peptide synthesis, RP-HPLC, and MS; eight figures showing HPLC chromatograms and mass spectra that show the purity of cyclic NGR peptides as well as their chemostability and decomposition under different conditions. This material is available free of charge via the Internet at http://pubs.acs.org.

■ AUTHOR INFORMATION

Corresponding Author

*E-mail gmezo@elte.hu; tel +36-1-372-2500/1433; fax +36-1-372-2620.

Notes

The authors declare no competing financial interest.

DOI: 10.1021/jm501630j
J. Med. Chem. 2015, 58, 1806−1817

■ ACKNOWLEDGMENTS

This work was supported by grants from the Hungarian National Science Fund (OTKA, K 104045, K 100720, and NK 101072) and by the Hungarian National Brain Research Program (KTIA_NAP_13-2014-0009, Hungary).

■ ABBREVIATIONS USED

Acm, acetamidomethyl; Asu, aspartimide; Boc, *tert*-butyloxycarbonyl; BOP, (benzotriazol-1-yloxy)tris(dimethylamino)-phosphonium hexafluorophosphate; ClAc-OPcp, chloroacetic acid pentachlorophenyl ester; ClZ, 2-chlorobenzyloxycarbonyl; DIC, *N*,*N*′-diisopropylcarbodiimide; DIEA, *N*,*N*-diisopropylethylamine; DMEM, Dulbecco's modified Eagle's medium; DQF-COSY, double quantum filtered correlation spectroscopy; FCS, fetal calf serum; Fmoc, fluorenylmethyloxycarbonyl; HOBt, 1-hydroxybenzotriazole; IFNγ, interferon γ; MBHA, 4-methylbenzhydrylamine; ROESY, rotating-frame Overhauser spectroscopy; RP, reverse phase; RPMI, Roswell Park Memorial Institute medium; TFE, 2,2,2-trifluoroethanol; TIS, triisopropylsilane; Tl(tfa)$_3$, thallium trifluoroacetate; TOCSY, total correlation spectroscopy

■ REFERENCES

(1) Koivunen, E.; Wang, B.; Ruoslahti, E. Isolation of highly specific ligand for the alpha 5 beta 1 integrin from a phage display library. *J. Cell Biol.* **1994**, *124*, 373−380.

(2) Healy, J. M.; Murayama, O.; Maeda, T.; Yoshino, K.; Sekiguchi, K.; Kikuchi, M. Peptide ligands for integrin alpha v beta 3 selected from random phage display libraries. *Biochemistry* **1995**, *34*, 3948−3955.

(3) Arap, W.; Pasqualini, R.; Ruoslahti, E. Cancer treatment by targeted drug delivery to tumor vasculature in a mouse model. *Science* **1998**, *279*, 377−380.

(4) Pasqualini, R.; Koivunen, E.; Kain, R.; Lahdenranta, J.; Sakamoto, M.; Stryhn, A.; Ashmun, R. A.; Shapiro, L. H.; Arap, W.; Ruoslahti, E. Aminopeptidase N is a receptor for tumor-homing peptides and a target for inhibiting angiogenesis. *Cancer Res.* **2000**, *60*, 722−727.

(5) Curnis, F.; Arrigoni, G.; Sacchi, A.; Fischetti, L.; Arap, W.; Pasqualini, R.; Corti, A. Differential binding of drugs containing the NGR motif to CD13 isoforms in tumor vessels, epithelia and myeloid cells. *Cancer Res.* **2002**, *62*, 867−874.

(6) Luan, Y.; Xu, W. The structure and main functions of aminopeptidase N. *Curr. Med. Chem.* **2007**, *14*, 639−647.

(7) Corti, A.; Curnis, F.; Arap, W.; Pasqualini, R. The neovasculature homing motif NGR: More than meets the eye. *Blood* **2008**, *112*, 2628−2635.

(8) Corti, A.; Curnis, F. Tumor vasculature targeting through NGR-peptide-based drug delivery systems. *Curr. Pharm. Biotechnol.* **2011**, *12*, 1128−1134.

(9) Wickström, M.; Larsson, R.; Nygren, P.; Gullbo, J. Aminopeptidase N (CD13) as a target for cancer chemotherapy. *Cancer Sci.* **2011**, *102*, 501−508.

(10) Geiger, T.; Clarke, S. Deamidation, isomerisation, and racemisation at asparaginyl and aspartyl residues in peptides. *J. Biol. Chem.* **1987**, *262*, 785−794.

(11) Stephenson, R. C.; Clarke, S. Succinimide formation from aspartyl and asparaginyl peptides as a model for the spontaneous degradation of proteins. *J. Biol. Chem.* **1989**, *264*, 6164−6170.

(12) Tyler-Cross, R.; Schirch, V. Effects of amino acid sequence, buffers, and ionic strength on the rate and mechanism of deamidation of asparagine residues in small peptides. *J. Biol. Chem.* **1991**, *266*, 22549−22556.

(13) Patel, K.; Borchardt, R. T. Chemical pathways of peptide degradation. III. Effect of primary sequence on pathways of deamidation of asparaginyl residues in hexapeptide. *Pharm. Res.* **1990**, *7*, 787−793.

(14) Stevenson, C. L.; Friedman, A. R.; Kubiak, T. M.; Donlan, M. E.; Borchardt, R. T. Effect of secondary structure on the rate of deamidation of several growth hormone releasing factor analogs. *Int. J. Pept. Protein Res.* **1993**, *42*, 497−503.

(15) Xie, M.; Schowen, R. L. Secondary structure and protein deamidation. *J. Pharm. Sci.* **1999**, *88*, 8−13.

(16) Xie, M.; Aube, J.; Borchardt, R. T.; Morton, M.; Topp, E. M.; Vandar Velde, D.; Schowen, R. L. Reactivity toward deamidation of asparagine residues in beta-turn structures. *J. Pept. Res.* **2000**, *56*, 165−171.

(17) Capasso, S.; Balboni, G.; Di Cerbo, P. Effect of lysine residues on the deamidation reaction of asparagine side chain. *Biopolymers* **2000**, *53*, 213−219.

(18) Plesniak, L. A.; Salzameda, B.; Hinderberger, H.; Regan, E.; Kahn, J.; Mills, S. A.; Teriete, P.; Yao, Y.; Jennings, P.; Marassi, F.; Adams, J. A. Structure and activity of CPNGRC: A modified CD13/APN peptidic homing motif. *Chem. Biol. Drug Des.* **2010**, *75*, 551−562.

(19) Curnis, F.; Cattaneo, A.; Longhi, R.; Sacchi, A.; Gasparri, A. M.; Pastorino, F.; Di Matteo, P.; Traversari, C.; Bachi, A.; Ponzoni, M.; Rizzardi, G. P.; Corti, A. Critical role of flanking residues in NGR-to-isoDGR transition and CD13/integrin receptor switching. *J. Biol. Chem.* **2010**, *285*, 9114−9123.

(20) Wakankar, A. A.; Borchardt, R. T. Formulation considerations for proteins susceptible to asparagine deamidation and aspartate isomerisation. *J. Pharm. Sci.* **2006**, *95*, 2321−2336.

(21) Curnis, F.; Sacchi, A.; Borgna, L.; Magni, F.; Gasparri, A.; Corti, A. Enhancement of tumor necrosis factor alpha antitumor immunotherapeutic properties by targeted delivery to aminopeptidase N (CD13). *Nat. Biotechnol.* **2000**, *18*, 1185−1190.

(22) Colombo, G.; Curnis, F.; De Mori, G. M.; Gasparri, A.; Longoni, C.; Sacchi, A.; Longhi, R.; Corti, A. Structure-activity relationship of linear and cyclic peptides containing NGR tumor-homing motif. *J. Biol. Chem.* **2002**, *277*, 47891−47897.

(23) Sacchi, A.; Gasparri, A.; Curnis, F.; Bellone, M.; Corti, A. Crucial role for interferon gamma in the synergism between tumor vasculature-targeted tumor necrosis alpha (NGR-TNF) and doxorubicin. *Cancer Res.* **2004**, *64*, 7150−7155.

(24) Curnis, F.; Gasparri, A.; Sacchi, A.; Cattaneo, A.; Magni, F.; Corti, A. A target delivery of IFNgamma to tumor vessels uncouples antitumor from counterregulatory mechanism. *Cancer Res.* **2005**, *65*, 2906−2913.

(25) Crippa, L.; Gasparri, A.; Sacchi, A.; Ferrero, E.; Curnis, F.; Corti, A. Synergistic damage of tumor vessels with ultra low-dose endothelial-monocyte activating polypeptide-II and neovasculature-targeted tumor necrosis factor-alpha. *Cancer Res.* **2008**, *68*, 1154−1161.

(26) Pastorino, F.; Brignole, C.; Marimpietri, D.; Cilli, M.; Gambini, C.; Ribatti, D.; Longhi, R.; Allen, T. M.; Corti, A.; Ponzoni, M. Vascular damage and anti-angiogenic effects of tumor vessel-targeted liposomal chemotherapy. *Cancer Res.* **2003**, *63*, 7400−7409.

(27) Pastorino, F.; Brignole, C.; Di Paolo, D.; Nico, B.; Pezzolo, A.; Marimpietri, D.; Pagnan, G.; Piccardi, F.; Cilli, M.; Longhi, R.; Ribatti, D.; Corti, A.; Allen, T. M.; Ponzoni, M. Targeting liposomal chemotherapy via both tumor cell-specific and tumor vasculature-specific ligands potentiates therapeutic efficacy. *Cancer Res.* **2006**, *66*, 10073−10082.

(28) Ndinguri, M. W.; Solipuram, R.; Gambrell, R. P.; Aggarwal, S.; Hammer, R. P. Peptide targeting of platinum anti-cancer drugs. *Bioconjugate Chem.* **2009**, *20*, 1869−1878.

(29) Luo, L. M.; Huang, Y.; Zhao, B. X.; Zhao, X.; Duan, Y.; Du, R.; Yu, K. F.; Song, P.; Zhao, Y.; Zhang, X.; Zhang, Q. Anti-tumor and anti-angiogenic effect of metronomic cyclic NGR-modified liposomes containing paclitaxel. *Biomaterials* **2013**, *34*, 1102−1114.

(30) Chen, K.; Ma, W.; Li, G.; Wang, J.; Yang, W.; Yap, L. P.; Hughes, L. D.; Park, R.; Conti, P. S. Synthesis and evaluation of ^{64}Cu-labeled monomeric and dimeric NGR-peptides for MicroPET imaging of CD13 receptor expression. *Mol. Pharmaceutics* **2013**, *10*, 417−427.

(31) Ma, W.; Kang, F.; Wang, Z.; Yang, W.; Li, G.; Ma, X.; Li, G.; Chen, K.; Zhang, Y.; Wang, J. (99m)Tc-labeled monomeric and

DOI: 10.1021/jm501630j
J. Med. Chem. 2015, 58, 1806−1817

dimeric NGR-peptides for SPECT imaging of CD13 receptor in tumor-bearing mice. *Amino Acids* **2013**, *44*, 1337−1345.
(32) Dunn, M.; Zheng, J.; Rosenblat, J.; Jaffray, D. A.; Allen, C. APN/CD13-targeting as a strategy to alter the tumor accumulation of liposomes. *J. Controlled Release* **2011**, *154*, 298−305.
(33) Negussie, A. H.; Miller, J. L.; Reddy, G.; Drake, S. K.; Wood, B. J.; Dreher, M. R. Synthesis and in vitro evaluation of cyclic NGR-peptide targeted thermally sensitive liposome. *J. Controlled Release* **2010**, *143*, 265−273.
(34) Corti, A.; Ponzoni, M. Tumor vascular targeting with tumor necrosis factor alpha and chemotherapeutic drugs. *Signal Transduction Commun. Cancer Cells* **2004**, *1028*, 104−112.
(35) Marelli, U. K.; Rechenmacher, F.; Sobahi, T. R.; Mas-Moruno, C.; Kessler, H. Tumor targeting via integrin ligands. *Front. Oncol.* **2013**, *3*, No. 222.
(36) Zou, M.; Zhang, L.; Xie, Y.; Xu, W. NGR-based strategies for targeting delivery of chemotherapeutics to tumor vasculature. *Anticancer Agents Med. Chem.* **2012**, *12*, 239−246.
(37) Tugyi, R.; Mező, G.; Fellinger, E.; Andreu, D.; Hudecz, F. The effect of cyclization on the enzymatic degradation of herpes simplex virus glycoprotein D derived epitope peptide. *J. Pept. Sci.* **2005**, *11*, 642−649.
(38) Jakab, A.; Schlosser, G.; Feijlbrief, M.; Welling-Wester, S.; Manea, M.; Vila-Perello, M.; Andreu, D.; Hudecz, F.; Mező, G. Synthesis and antibody recognition of cyclic epitope peptides, together with their dimer and conjugated derivatives based on residues 9−22 of herpes simplex virus type 1 glycoprotein D. *Bioconjugate Chem.* **2009**, *20*, 683−692.
(39) Perczel, A.; Hollósi, M. Turns. In *Circular Dichroism and the Conformational Analysis of Biomolecules*; Fasman, G. D., Ed.; Plenum Press: New York, 1996; pp 285−380.
(40) Vass, E.; Majer, Zs.; Kőhalmy, K.; Hollósi, M. Vibrational and chiroptical spectroscopic characterization of γ-turn model cyclic tetrapeptides containing two β-Ala residues. *Chirality* **2010**, *22*, 762−771.
(41) Povey, J. F.; Smales, C. M.; Hassard, S. J.; Howard, M. J. Comparison of the effect of 2,2,2-trifluoroethanol on peptide and protein structure and function. *J. Struct. Biol.* **2007**, *157*, 329−338.
(42) Bürgi, H. B.; Dunitz, J. D.; Lehn, J. M.; Wipff, G. Stereochemistry of reaction paths at carbonyl centres. *Tetrahedron* **1974**, *30*, 1563−1572.
(43) Perczel, A.; Ángyán, J. G.; Kajtár, M.; Viviani, W.; Rivail, J. L.; Marcoccia, J. F.; Csizmadia, I. G. Peptide models 1. Topology of selected peptide conformational potential-energy surfaces (glycine and alanine derivatives). *J. Am. Chem. Soc.* **1991**, *113*, 6256−6265.
(44) Spitaleri, A.; Mari, S.; Curnis, F.; Traversari, C.; Longhi, R.; Bordignon, C.; Corti, A.; Rizzardi, G. P.; Musco, G. Structural basis for the interaction of isoDGR with the RGD-binding site of alphavbeta3 integrin. *J. Biol. Chem.* **2008**, *283*, 19757−19768.
(45) Bochen, A.; Marelli, U. K.; Otto, E.; Pallarola, D.; Mas-Moruno, C.; Di Leva, F. S.; Boehm, H.; Spatz, J. P.; Novellino, E.; Kessler, H.; Marinelli, L. Biselectivity of isoDGR peptides for fibronectin binding integrin subtypes α5β1 and αvβ6: Conformational control through flanking amino acids. *J. Med. Chem.* **2013**, *56*, 1509−1519.
(46) Aznavoorian, S.; Stracke, M. L.; Krutzsch, H.; Schiffmann, E.; Liotta, L. A. Signal transduction for chemotaxis and haptotaxis by matrix molecules in tumor cells. *J. Cell Biol.* **1990**, *110*, 1427−1438.
(47) Soudy, R.; Ahmed, S.; Kaur, K. NGR-peptide ligands for targeting CD13/APN identified through peptide array screening resemble fibronectin sequences. *ACS Comb. Sci.* **2012**, *14*, 590−599.
(48) Vranken, W. F.; Boucher, W.; Stevens, T. J.; Fogh, R. H.; Pajon, A.; Llinas, M.; Ulrich, E. L.; Markley, J. L.; Ionides, J.; Laue, E. D. The CCPN data model for NMR spectroscopy: Development of a software pipeline. *Proteins: Struct., Funct., Bioinf.* **2005**, *59*, 687−696.
(49) Brunger, A. T.; Adams, P. D.; Clore, G. M.; Gros, P.; Grosse-Kunstleve, R. W.; Jiang, J. S.; Kuszewski, J.; Nilges, N.; Pannu, N. S.; Read, R. J.; Rice, L. M.; Simonson, T.; Warren, G. L. Crystallography & NMR System (CNS), a new software suite for macromolecular structure determination. *Acta Crystallogr.* **1998**, *D54*, 905−921.
(50) Brunger, A. T. Version 1.2 of the Crystallography and NMR System. *Nat. Protoc.* **2007**, *2*, 2728−2733.
(51) Todaro, G. J.; Fryling, C.; De Larco, J. E. Transforming growth factors produced by certain human tumor cells: polypeptides that interact with epidermal growth factor receptors. *Proc. Natl. Acad. Sci. U.S.A.* **1980**, *77*, 5258−5262.
(52) Lajkó, E.; Szabó, I.; Andódy, K.; Pungor, A.; Mező, G.; Kőhidai, L. Investigation on chemotactic drug targeting (chemotaxis and adhesion) inducer effect of GnRH-III derivatives in *Tetrahymena* and human leukemia cell line. *J. Pept. Sci.* **2013**, *19*, 46−58.

DOI: 10.1021/jm501630j
J. Med. Chem. 2015, 58, 1806−1817